AMERICAN SOCIETY FOR MICROBIOLOGY | Journal of Virology®

PRIONS

Robust Central Nervous System Pathology in Transgenic Mice following Peripheral Injection of α-Synuclein Fibrils

Jacob I. Ayers,[a,b,c] Mieu M. Brooks,[a,b] Nicola J. Rutherford,[a,b] Jasie K. Howard,[a,b] Zachary A. Sorrentino,[a,b] Cara J. Riffe,[a,b] Benoit I. Giasson[a,b,c]

Department of Neuroscience,[a] Center for Translational Research in Neurodegenerative Disease,[b] McKnight Brain Institute,[c] University of Florida, Gainesville, Florida, USA

ABSTRACT Misfolded α-synuclein (αS) is hypothesized to spread throughout the central nervous system (CNS) by neuronal connectivity leading to widespread pathology. Increasing evidence indicates that it also has the potential to invade the CNS via peripheral nerves in a prion-like manner. On the basis of the effectiveness following peripheral routes of prion administration, we extend our previous studies of CNS neuroinvasion in M83 αS transgenic mice following hind limb muscle (intramuscular [i.m.]) injection of αS fibrils by comparing various peripheral sites of inoculations with different αS protein preparations. Following intravenous injection in the tail veins of homozygous M83 transgenic ($M83^{+/+}$) mice, robust αS pathology was observed in the CNS without the development of motor impairments within the time frame examined. Intraperitoneal (i.p.) injections of αS fibrils in hemizygous M83 transgenic ($M83^{+/-}$) mice resulted in CNS αS pathology associated with paralysis. Interestingly, injection with soluble, nonaggregated αS resulted in paralysis and pathology in only a subset of mice, whereas soluble Δ71-82 αS, human βS, and keyhole limpet hemocyanin (KLH) control proteins induced no symptoms or pathology. Intraperitoneal injection of αS fibrils also induced CNS αS pathology in another αS transgenic mouse line (M20), albeit less robustly in these mice. In comparison, i.m. injection of αS fibrils was more efficient in inducing CNS αS pathology in M83 mice than i.p. or tail vein injections. Furthermore, i.m. injection of soluble, nonaggregated αS in $M83^{+/-}$ mice also induced paralysis and CNS αS pathology, although less efficiently. These results further demonstrate the prion-like characteristics of αS and reveal its efficiency to invade the CNS via multiple routes of peripheral administration.

IMPORTANCE The misfolding and accumulation of α-synuclein (αS) inclusions are found in a number of neurodegenerative disorders and is a hallmark feature of Parkinson's disease (PD) and PD-related diseases. Similar characteristics have been observed between the infectious prion protein and αS, including its ability to spread from the peripheral nervous system and along neuroanatomical tracts within the central nervous system. In this study, we extend our previous results and investigate the efficiency of intravenous (i.v.), intraperitoneal (i.p.), and intramuscular (i.m.) routes of injection of αS fibrils and other protein controls. Our data reveal that injection of αS fibrils via these peripheral routes in αS-overexpressing mice are capable of inducing a robust αS pathology and in some cases cause paralysis. Furthermore, soluble, nonaggregated αS also induced αS pathology, albeit with much less efficiency. These findings further support and extend the idea of αS neuroinvasion from peripheral exposures.

KEYWORDS alpha-synuclein, Lewy pathology, peripheral, prions, transgenic mice

Received 21 October 2016 **Accepted** 4 November 2016

Accepted manuscript posted online 16 November 2016

Citation Ayers JI, Brooks MM, Rutherford NJ, Howard JK, Sorrentino ZA, Riffe CJ, Giasson BI. 2017. Robust central nervous system pathology in transgenic mice following peripheral injection of α-synuclein fibrils. J Virol 91:e02095-16. https://doi.org/10.1128/JVI.02095-16.

Editor Byron Caughey, Rocky Mountain Laboratories

Address correspondence to Jacob I. Ayers, jacob.ayers@mbi.ufl.edu, or Benoit I. Giasson, bgiasson@ufl.edu.

A spectrum of neurodegenerative diseases associated with the formation of brain amyloidogenic inclusions comprised of the protein α-synuclein (αS) are collectively referred to as α-synucleinopathies (1–6). αS pathological inclusions, which are also termed Lewy bodies or Lewy neurites, predominantly occur in neurons and are a defining feature of Parkinson's disease (PD) (1–7), but in other diseases such as multiple system atrophy, they can predominantly occur in oligodendrocytes (6, 8–10). A direct role for αS in neurodegeneration was established by the discovery of several genetic alterations in the αS gene (*SNCA*), in the form of missense mutations or increased copy number, which result in autosomal-dominant PD or the related disease, dementia with Lewy bodies (11–21).

Human pathological studies have suggested that αS pathology may spread within the central nervous system (CNS) along neuroanatomical tracts (22–24) and perhaps from the peripheral nervous system (PNS) (22, 25, 26). Using either human or mouse brain lysates containing αS aggregates or recombinant preformed αS fibrils (αS fibs), it was reported that the brain injection of these preparations could result in the progressive induction of αS pathology in αS transgenic (Tg) mice and in some studies in nontransgenic (nTg) mice (27–38). However, we have recently reported that the studies using CNS homogenates can be confounded by a non-αS factor enriched in the white matter that can induce similar αS pathology in αS Tg mice (39). We previously reported that, consistent with a prion-like mechanism, peripheral hind limb intramuscular (i.m.) injection of αS fibs leads to the progressive formation of CNS αS pathology in both M20 and M83 αS Tg mice and to motor impairment in the latter line of mice (40). Retrograde transport of αS aggregates followed by seeding and further transmission was suggested as the major mechanism involved, as transection of the sciatic nerve prior to i.m. injection of αS fibs significantly delayed, but did not completely block, disease induction in this model (40). Herein, we expand these studies of CNS induction of αS pathology from peripheral challenges of αS fibs and control proteins by comparing the outcomes of tail vein, intraperitoneal (i.p.) and i.m. inoculations.

RESULTS

We previously reported that the unilateral or bilateral i.m. injection in the hind limbs of M83 αS Tg mice with mouse or human αS fibs resulted in the formation of CNS αS pathology associated with a severe motor impairment (40). To demonstrate that neuroinvasion of the injected αS fibs could occur via retrograde transport through the sciatic nerve (the major nerve that innervates the lower leg muscles), we had performed complete transection of the sciatic nerve prior to unilateral i.m. injection of the αS fibs in the ipsilateral hind limb (40). Sciatic nerve transection significantly delayed disease onset in some of the mice, yet others developed the same phenotype and αS pathology as mice whose nerves were not transected (40). This revealed that neuroinvasion of αS aggregates could occur through retrograde transport via the nerve, but other mechanisms could also be involved.

To determine whether leakage of αS fibs into the vascular circulation could be another mechanism of neuroinvasion, we performed tail vein injection of 20 μg of mouse αS fibs in a cohort of five homozygous M83 Tg ($M83^{+/+}$) mice. This was the most common dose used in our previous i.m. injection studies (40). We used mouse αS fibs for these studies, as we previously showed that human or mouse αS fibs could be interchangeably used to induce αS pathology following i.m. injection in M83 mice, but mouse αS fibs were slightly more potent (40). Importantly, naive $M83^{+/+}$ mice intrinsically develop motor impairments associated with the CNS formation of αS inclusion pathology, but only after 7 months of age, and this is delayed beyond 21 months of age for hemizygous M83 Tg ($M83^{+/-}$) mice (41). $M83^{+/+}$ mice were injected in the tail vein at 2 months of age and monitored for 120 days thereafter. Although the $M83^{+/+}$ mice that were i.m. injected with 20 μg mouse αS fibs developed motor impairment (i.e., foot drop followed by paralysis) within 60 days postinjection (dpi) (40), tail vein-injected mice did not develop a motor impairment phenotype within the 120 days that they were monitored following injection. However, four out of five of these mice had

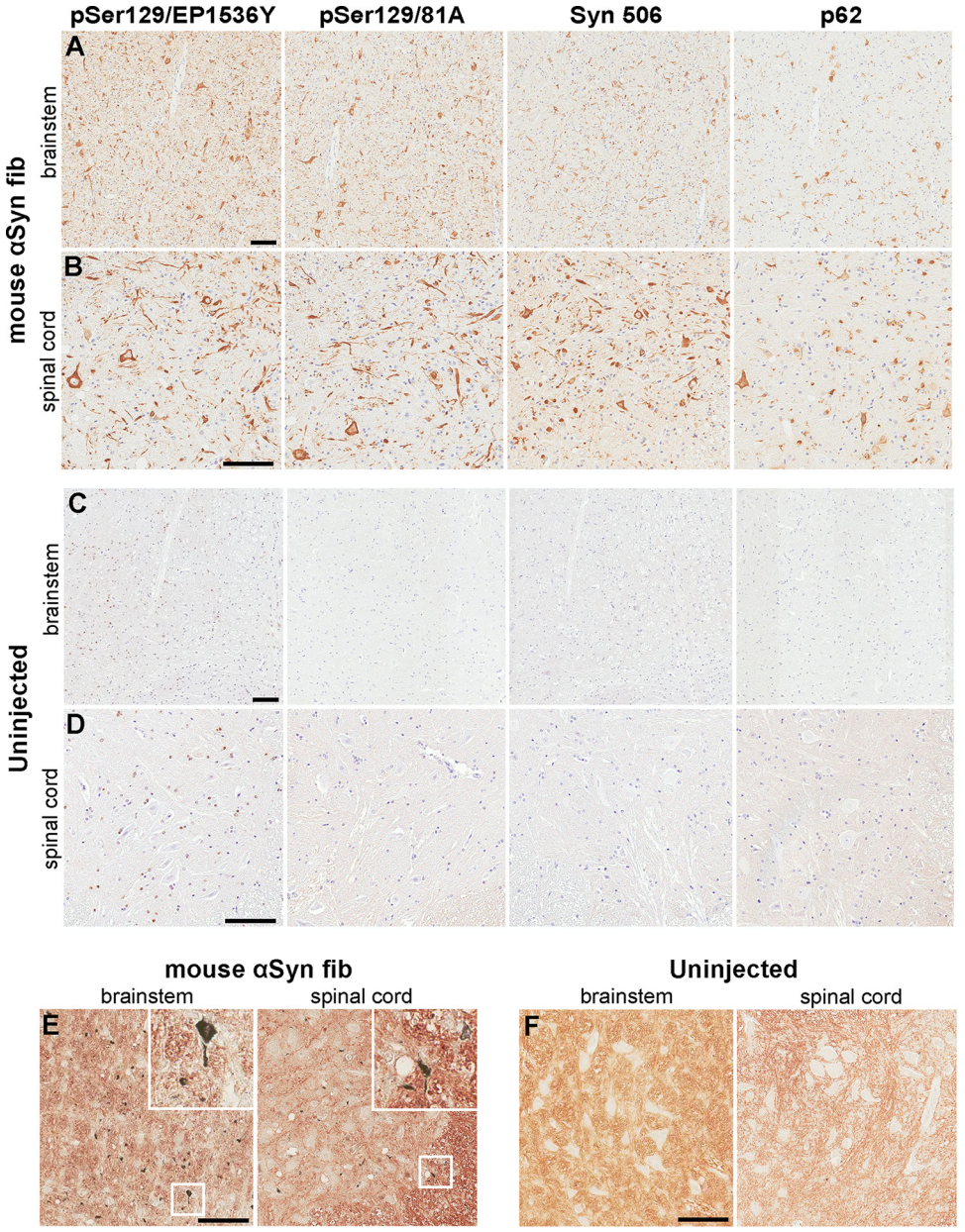

FIG 1 Induction of CNS αS inclusion pathology in M83$^{+/+}$ mice following tail vein injection of αS fibs. (A and B) Representative images showing αS inclusion pathology in the brain stem (A) and spinal cord (B) of M83$^{+/+}$ mice injected in the tail vein with 20 μg mouse αS fibs. (C and D) Representative images show the lack of αS inclusion pathology in the brain stem (C) and spinal cord (D) of uninjected age-matched M83$^{+/+}$ mice. Tissue sections were stained with antibodies to αS phosphorylated at Ser129 (EP1536Y and 81A), anti-αS (Syn 506) or anti-p62/sequestosome (a general marker of inclusion pathology) as indicated in each panel. Tissue sections were counterstained with hematoxylin. (E and F) Representative images revealing the presence of argyrophilic deposits in the brain stems and spinal cords (as indicated by insets [×3 magnification]) of M83$^{+/+}$ mice injected in the tail vein with 20 μg mouse αS fibs (E), and a lack of deposits in age-matched uninjected M83$^{+/+}$ mice (F). Bars = 100 μm.

widespread αS inclusion pathology in the spinal cord, brain stem, midbrain, hypothalamus, thalamus, and periaqueductal gray regions typical of the pathology that these mice present with due to aging (Fig. 1A and B) and displayed widespread argyrophilic deposits throughout the CNS (Fig. 1E) (41). The other mouse from this cohort had a similar distribution of αS pathology, but a more modest density. Additionally, uninjected M83$^{+/+}$ mice at 180 days displayed no αS pathology or argyrophilic deposits throughout their CNS (Fig. 1C, D, and F).

TABLE 1 Summary of the M83$^{+/-}$ mice i.p. injected

Inoculum[a]	Predetermined endpoint (dpi)	No. of animals paralyzed/no. injected	No. of animals with αS pathology/no. analyzed	CNS distribution of αS pathology[b]
mfib αS	180	3/6[c]	6/6	Predominantly thalamus, hypothalamus, periaqueductal gray, brain stem, and SC
Mouse soluble αS	180	1/11	2/11	Predominantly thalamus, hypothalamus, periaqueductal gray, brain stem, and SC
Human Δ71-82 αS	180	0/10	0/10	None
Human βS	210	0/6	0/6	None
KLH	200	0/5	0/5	None

[a]mfib, mouse αS fibs; KLH, keyhole limpet hemocyanin.
[b]SC, spinal cord.
[c]One mouse had to be euthanized for non-motor-impaired health complications (169 dpi).

To extend these studies, i.p. administration of αS fibs was performed in M83$^{+/-}$ mice in addition to a series of control proteins. Intraperitoneal injection with 50 μg of mouse αS fibs resulted in severe motor impairment in three out of six mice by 180 days (Table 1; Fig. 2A). One additional mouse had to be euthanized at 169 dpi due to dermatitis, while the other two mice were euthanized at 180 dpi without a motor phenotype. Similar to tail vein injections, 5 of these mice had widespread CNS αS inclusion pathology (Table 1; Fig. 3A and B), while the sixth had αS pathology with similar distribution, but at more modest levels. For controls, we i.p. injected M83$^{+/-}$ mice with nonaggregated, soluble mouse αS that was sedimented at high speed just prior to injection to remove any possible aggregates. From this cohort of 11 mice, 1 developed motor impairment similar to mice injected with mouse αS fibs and presented with similar αS inclusion pathology (Table 1; Fig. 2A and 3C and D). The remaining 10 mice were disease-free up to 180 dpi, the time at which they were euthanized. Of the 10 disease-free mice, only 1 had moderate αS pathology with the same distribution as those previously described, while the other 9 had no αS inclusion pathology.

Ten M83$^{+/-}$ mice were i.p. injected with 50 μg of soluble αS containing the Δ71-82 (amino acids 71 to 82 deleted) deletion. This nonamyloidogenic protein has a deletion in a region required for αS to aggregate and form amyloid (42, 43). Δ71-82 αS lacks the ability to form or seed αS amyloid *in vitro* and in cultured cells under relatively physiologic conditions (42–45). None of the M83$^{+/-}$ mice i.p. injected with Δ71-82 αS developed a motor impairment phenotype or presented with αS inclusion pathology at 180 dpi, the time at which they were euthanized (Table 1; Fig. 2A and 3E). Six M83$^{+/-}$ mice were i.p. injected with βS, a closely related protein to αS (46), but because of

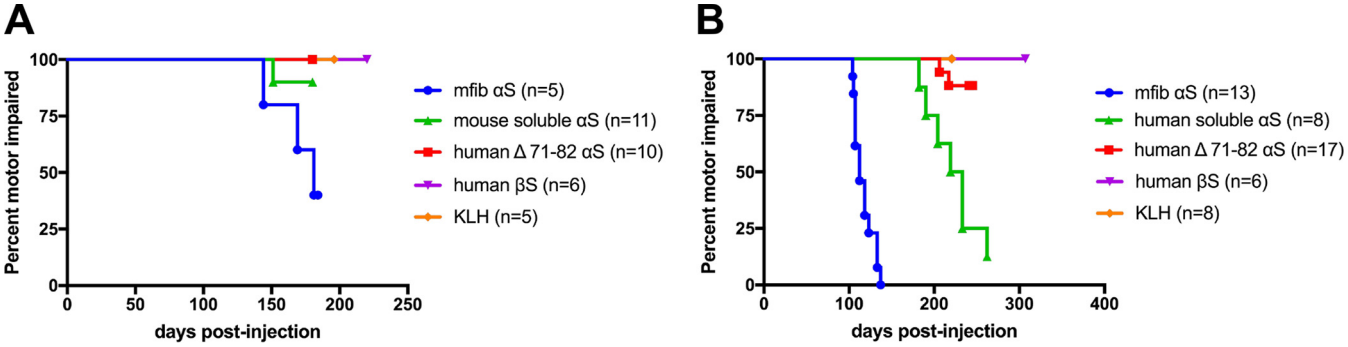

FIG 2 Induction of motor impairments and paralysis in M83$^{+/-}$ mice peripherally challenged with various forms of αS. (A) Kaplan-Meier survival plot shows a decreased time to end stage (due to motor impairments) for M83$^{+/-}$ Tg mice injected i.p. with mouse αS fibs compared to M83$^{+/-}$ mice injected i.p. with Δ71-82 αS, soluble nonaggregated mouse αS, βS, or KLH. A mouse euthanized at an earlier time point due to a non-disease-related complication (i.e., dermatitis) was excluded from the data. mfib, mouse αS fib. (B) Bilateral i.m. injection in the hind limb muscle of M83$^{+/-}$ Tg mice with mouse αS fibs resulted in paralysis in all of the mice by 134 dpi. i.m. injections with soluble, nonaggregated human αS also resulted in the majority of animals developing paralysis, whereas only 2 of the 17 mice injected with Δ71-82 αS developed disease, and none of the mice injected with βS, or KLH ever displayed symptoms. Mice euthanized at earlier time points due to non-disease-related complications (i.e., fighting wounds) were excluded from these data (Table 1).

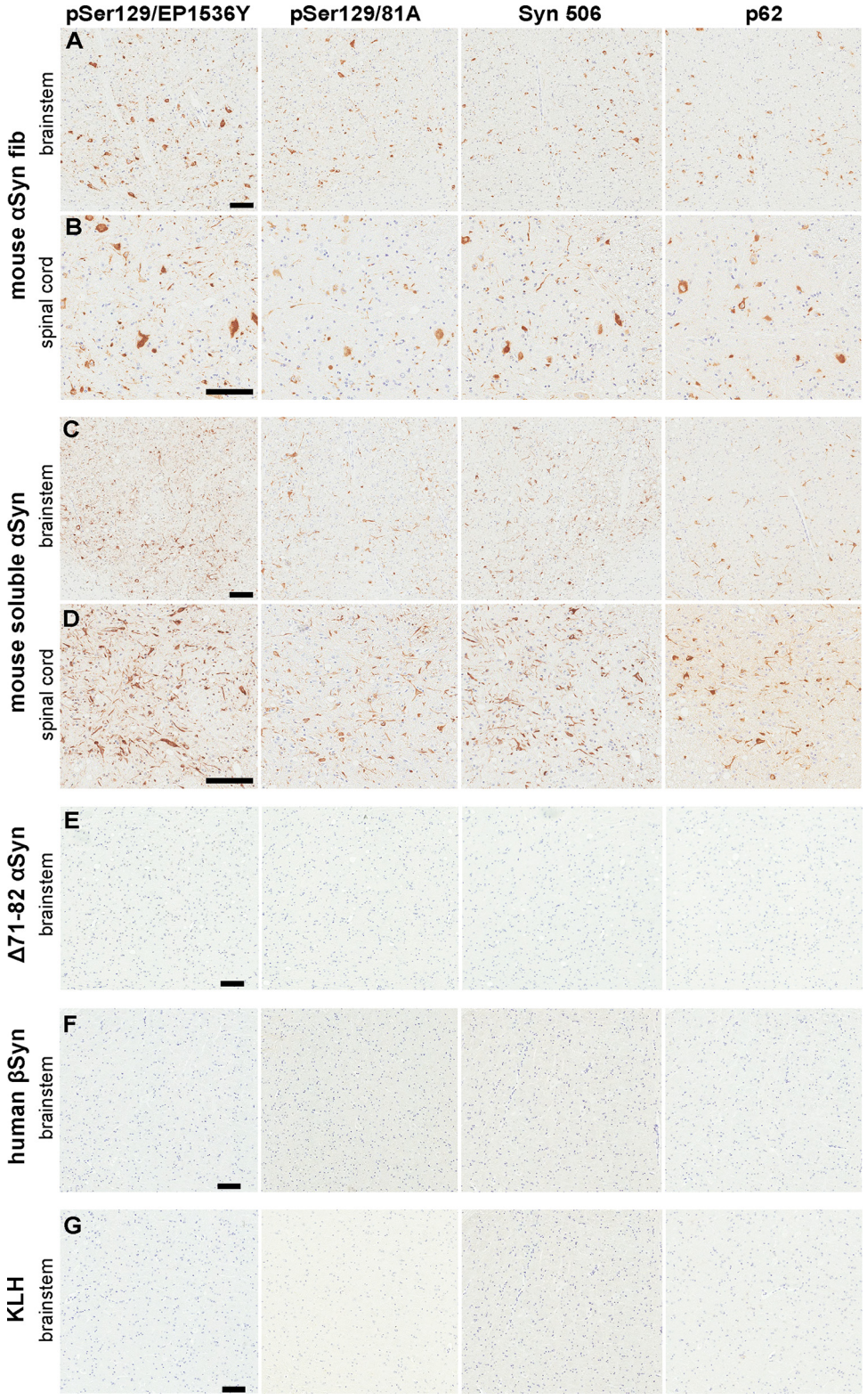

FIG 3 Induction of CNS αS inclusion pathology in M83$^{+/-}$ mice following i.p. injection of αS. (A and B) Representative images showing αS inclusion pathology in the brain stem (A) and spinal cord (B) of M83$^{+/-}$ mice i.p. injected with 50 μg mouse αS fibs. (C and D) Representative images showing αS inclusion pathology in the brain stem (C) and spinal cord (D) of M83$^{+/-}$ mice i.p. injected with 50 μg soluble mouse αS that developed motor impairments. (E to G) Representative images showing a paucity of αS inclusion pathology in the brain stems of M83$^{+/-}$ mice i.p. injected with 50 μg of Δ71-82 αS (E), βS (F), or KLH (G). Tissue sections were stained with antibodies to αS phosphorylated at Ser129 (EP1536Y and 81A), anti-αS (Syn 506), or anti-p62/sequestosome (a general marker of inclusion pathology) as indicated in each panel. Tissue sections were counterstained with hematoxylin. Bars = 100 μm.

differences in its middle hydrophobic region, it is resistant to amyloid formation and is not found within human brain inclusions (7, 9, 42, 47, 48). None of the mice i.p. injected with βS developed a motor impairment phenotype or presented with αS inclusion pathology at 210 dpi, the time at which they were euthanized (Table 1; Fig. 2A and 3F). For an additional control for general immune activation due to i.p. injection of a protein, we injected five M83$^{+/-}$ mice with 50 μg of keyhole limpet hemocyanin (KLH), a protein known to be highly immunogenic. None of these mice developed a motor phenotype or presented with αS inclusion pathology at 200 dpi, the time at which they were euthanized (Table 1; Fig. 2A and 3G).

To determine whether i.p. injection of mouse αS fibs could induce CNS αS inclusion pathology in a different αS Tg mouse line, we performed a similar injection in five M20$^{+/-}$ Tg mice. M20 αS Tg mice were generated similarly to the M83 line with the mouse prion protein promoter driving expression, but they express wild-type human αS rather than human αS containing the A53T mutation (41). Additionally, they express similar or higher levels of human αS with neuroanatomical distribution similar to that of M83 mice, but they never intrinsically develop a motor impairment phenotype or αS inclusion pathology (37, 41, 49). None of the M20$^{+/-}$ i.p. injected with αS fibs become paralyzed like the M83$^{+/-}$ mice, but they presented with variable levels of CNS αS pathology. We sacrificed one of the i.p. injected M20$^{+/-}$ mice at 230 dpi and observed rare αS inclusions in the spinal cord and brain stem. Three of the four remaining mice had to be euthanized at 343, 343, and 365 dpi due to difficulty breathing or moribund state, and they presented with abundant αS inclusion pathology in the spinal cord and moderate levels in the brain stem and midbrain region (Fig. 4). The fifth mouse was euthanized at 365 dpi without a phenotype, but had scant αS inclusion pathology in the spinal cord and brain stem. Importantly, uninjected M20$^{+/-}$ mice at 450 days displayed no αS pathology in their CNS (Fig. 4C and D).

In our original study of i.m. injection of αS fibs in M83 mice, we showed that injections with either human or mouse αS fibs yield similar results and that i.m. injection of Δ71-82 αS could induce αS inclusion pathology and motor impairments in a subset of these mice (40), a finding seemingly at odds with the i.p. injection studies here. First, we bilaterally i.m. injected 20 μg of mouse αS fibs in a cohort of 17 M83$^{+/-}$ mice. Although 4 of the mice from this cohort had to be euthanized due to non-motor-related issues, the other 13 mice all developed motor impairments within 134 dpi (Table 2; Fig. 2B and 5A and B). Upon examination of their CNS, all 17 of the mice had the expected presentation of CNS αS inclusion pathology (Table 2; Fig. 5A and B). We bilaterally i.m. injected 17 M83$^{+/-}$ mice with 20 μg of soluble Δ71-82 αS and monitored these mice for up to 240 dpi. Two mice developed foot drop and paralysis with abundant CNS αS inclusion pathology before the designed endpoint (Table 2; Fig. 2B and 5E). Two additional mice that displayed no motor impairment phenotype had abundant CNS αS inclusion pathology, while another presented with modest αS inclusion pathology within the spinal cord. Thus, these findings corroborate our previous work (40).

For new controls, we i.m. injected cohorts of six and eight M83$^{+/-}$ mice with 20 μg of human βS and KLH, respectively, and monitored these mice for 220+ dpi. None of these mice developed a motor impairment phenotype or presented with CNS αS inclusion pathology (Table 2; Fig. 2B and 5F and G). Since i.m. injection of human Δ71-82 αS induced motor impairment and CNS αS pathology in a subset of mice, we performed similar i.m. injections with soluble, full-length human αS. We used human αS here to more directly compare the effects to Δ71-82 αS which is a deletion variant of human αS. To ensure there were no aggregates, the protein was centrifuged at high speed just prior to injection, and the supernatant was analyzed by K114 fluorometry. i.m. injections of this nonaggregated, soluble αS induced severe motor impairments with robust CNS αS inclusion pathology within 270 dpi in seven out of eight of this cohort of mice (Table 2; Fig. 2B and 5C and D).

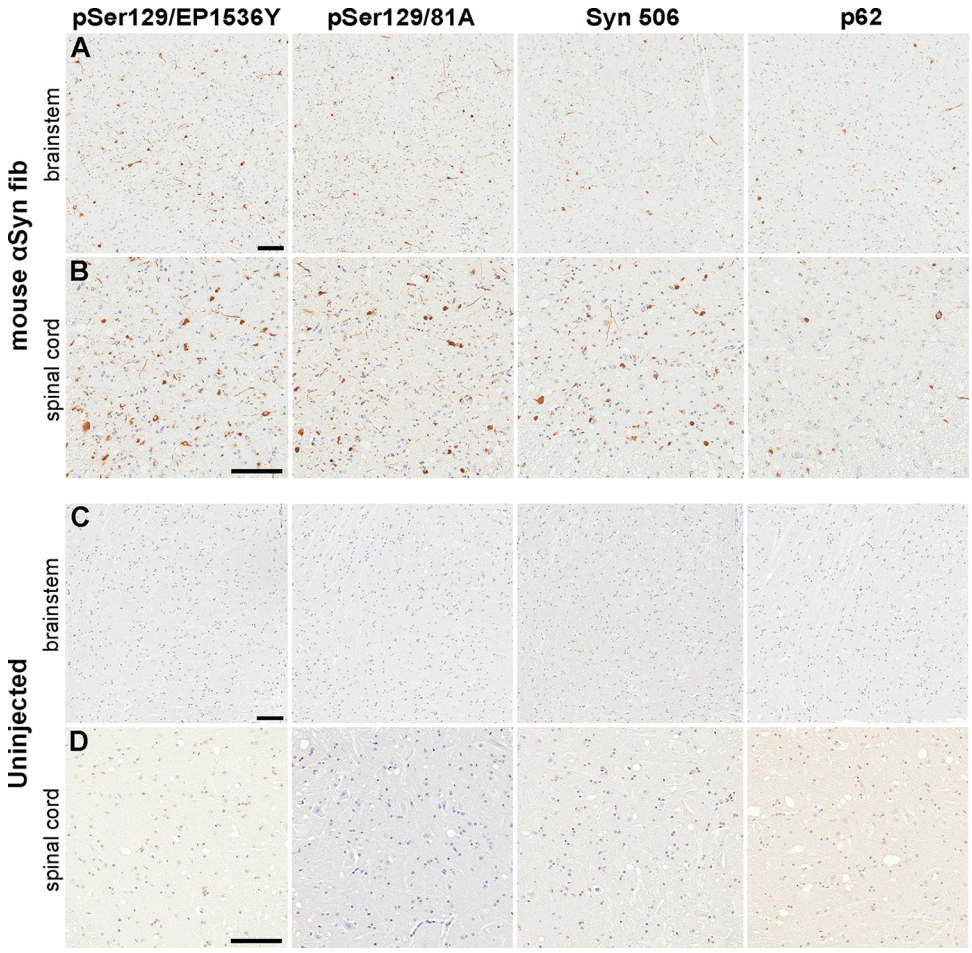

FIG 4 Induction of CNS αS inclusion pathology in M20$^{+/-}$ mice following i.p. injection of αS fibs. (A and B) Representative images showing αS inclusion pathology in the brain stem (A) and spinal cord (B) of M20$^{+/-}$ mice that were i.p. injected with 50 μg mouse αS fibs and developed a moribund state. (C and D) Representative images depicting a paucity of αS inclusion pathology in the brain stem (C) and spinal cord (D) of uninjected older (450 days) M20$^{+/-}$ mice. Tissue sections were stained with antibodies to αS phosphorylated at Ser129 (EP1536Y and 81A), anti-αS (Syn 506) or anti-p62/sequestosome (a general marker of inclusion pathology) as indicated in each panel. Tissue sections were counterstained with hematoxylin. Bars = 100 μm.

DISCUSSION

Our studies show that CNS αS pathology can be efficiently induced by peripheral exposure to amyloidogenic αS in M83 mice via i.m., i.p., or tail vein injections. The i.p. and tail vein injection studies do not directly provide a mechanism(s) for the CNS neuroinvasion following these types of exposure to exogenous αS amyloid seeds. However, the induction

TABLE 2 Summary of the M83$^{+/-}$ mice i.m. injected

Inoculum	Predetermined endpoint (dpi)	No. of animals paralyzed/no. injected	No. of animals with αS pathology/no. analyzed	CNS distribution of αS pathology
mfib αS	NA[a]	13/17[b]	17/17	Predominantly thalamus, hypothalamus, periaqueductal gray, brain stem, and SC
Human soluble αS	270	7/8[c]	7/8[c]	Predominantly thalamus, hypothalamus, periaqueductal gray, brain stem, and SC
Human Δ71-82 αS	240	2/17	5/17	Predominantly periaqueductal gray, brain stem, and SC. Sparse in thalamus and hypothalamus
Human βS	300	0/6	0/6	None
KLH	220	0/8	0/8	None

[a]NA, not applicable.
[b]Four mice had to be euthanized for non-motor-impaired health complications at 98, 107, 107, and 112 dpi (i.e., fighting wounds).
[c]One mouse had to be euthanized for non-motor-impaired health complications at 262 dpi (i.e., fighting wounds).

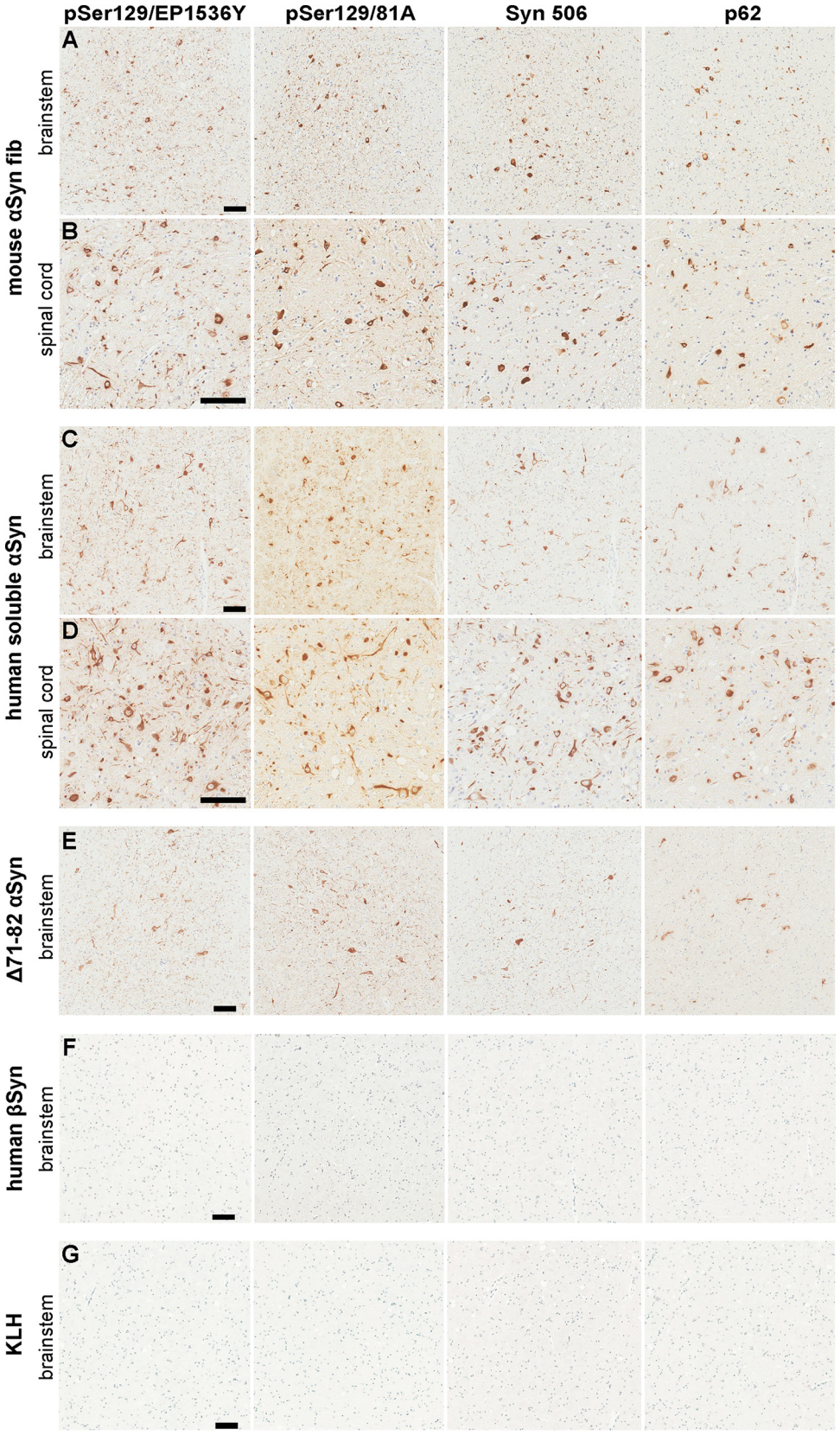

FIG 5 Induction of CNS αS inclusion pathology in M83$^{+/-}$ mice following i.m. injection of αS fibs and soluble αS. (A and B) Representative images showing αS inclusion pathology in the brain stem (A) and spinal cord (B) of M83$^{+/-}$ mice i.m. injected with 20 μg mouse αS fibs. (C and D) Representative images showing αS inclusion pathology in the brain stem (C) and spinal cord (D) of an M83$^{+/-}$ mouse that was i.m. injected with 20 μg soluble

(Continued on next page)

following tail vein injections suggested that these αS molecules can be taken up from the blood circulation to the nervous system. This finding can account for the previously reported incomplete inhibition of neuroinvasion by sciatic nerve transection following unilateral i.m. injection of the αS fibs in the ipsilateral hind limb (40).

Similar to our previous i.m. injection of αS fibs in M20$^{+/-}$ mice (40), i.p. injection of αS fibs in these mice also induced CNS αS pathology, but the induction/spread was slower than in M83 mice. Besides the M83 mice expressing A53T human αS and the M20 mice expressing wild-type human αS, it is possible that subtle expression differences in the periphery could contribute to these differences. i.p. injection of the control proteins Δ71-82 αS, βS, and KLH did not induce αS inclusion pathology in M83 mice. i.p. injection of soluble, nonaggregated αS was significantly less efficient at inducing αS pathology than αS fibs. Although this occurred in 2 out of the 11 injected mice, albeit only after prolonged incubation, it is possible that this preparation contained trace amounts of αS "seeds." Our findings support a recent study which also demonstrated the ability for αS fibrils, i.p. injected in transgenic mice expressing the A53T αS protein, to induce αS pathology and paralysis (50). Although the latter study provides insight into the potential efficiency of this peripheral route, we provide a higher powered study and include a number of control proteins which aim to better understand the component responsible for αS pathology and disease induction.

i.m. injections of βS and KLH in M83 mice also did not induce CNS αS inclusion pathology. The induction of CNS αS inclusion pathology by i.m. injection of αS fibs was similar to what we previously reported (40) as well as the ability of Δ71-82 αS to induce motor impairments and CNS αS inclusion pathology in a subset of mice. It was unexpected that i.m. injection of soluble, nonaggregated αS induced motor impairments and CNS αS inclusion pathology in the majority of M83$^{+/-}$ mice. It is possible that soluble, nonaggregated αS contains small amounts of αS seeds that cannot be removed even by high-speed centrifugation and that result in the induction of αS pathology following i.m. injection due to retrograde transport and conformational templating, a much more direct route to the CNS than the i.p. injection paradigm. The induction of disease and pathology by i.m. injection of Δ71-82 αS, which lacks the ability to form fibrils or seed αS amyloid *in vitro* and in cultured cells under relatively physiologic conditions (42–45), is more difficult to be explained by a conformational templating mechanism. Cerebral injections of Δ71-82 αS were previously shown to also have the ability to induce αS pathology in αS Tg mice, although with less efficiency than αS fibs (36, 37). However, the possibility that *in vivo*, a small amount of exogenous Δ71-82 αS might spontaneously acquire amyloidogenic properties over time cannot be excluded, since under nonphysiological conditions (i.e., the presence of SDS), it can be artificially induced to form amyloid fibrils (51). A more parsimonious explanation for the findings that soluble forms of αS can also induce αS pathology is that additional nonexclusive mechanisms, perhaps including immune activation, can contribute to inducing and/or promoting αS inclusion pathology formation (6, 52, 53).

The more efficient induction of CNS αS inclusion pathology from peripheral challenges with αS amyloid fibrils compared to soluble forms of αS and from i.m. injection compared to i.p. and tail vein injections indicates that CNS neuroinvasion associated with conformational templating of αS is still the predominant mechanism involved. This notion is consistent with the finding that tail vein injection of αS conformers in rats can induce the formation of morphologically distinct CNS αS pathology (54). It is also intriguing that in both the M83 and M20 mouse lines, the induced αS inclusion pathology always has

FIG 5 Legend (Continued)
human αS that developed motor impairments. (E) Representative images showing αS inclusion pathology in the brain stem of one of the M83$^{+/-}$ mice i.m. injected with 20 μg Δ71-82 αS that developed motor impairments. Paucity of αS inclusion pathology as shown in the brain stems of M83$^{+/-}$ mice i.m. injected with 20 μg βS (F) or KLH (G). Tissue sections were stained with antibodies to αS phosphorylated at Ser129 (EP1536Y and 81A), anti-αS (Syn 506), or anti-p62/sequestosome (a general marker of inclusion pathology) as indicated in each panel. Tissue sections were counterstained with hematoxylin. Bars = 100 μm.

the same general distribution, i.e., spinal cord, brain stem, midbrain, and thalamus regions, similar to that of naive M83 mice when they develop motor impairment with age. We speculate that this distribution is likely due to selective vulnerability, perhaps due to the mouse prion promoter used to drive the expression of αS in these transgenic mice. It is less likely that a specific mutual CNS neuroinvasion mechanism shared by these three different sites of peripheral inoculation (tail vein, gastrocnemius, and peritoneum) is the major cause of this distribution pattern, but we cannot exclude this possibility at this time.

In the current studies, we have not directly addressed the mechanism of CNS neuroinvasion from either i.p. or tail vein injections, but in the prion field, these routes of inoculation have been studied extensively, and it is believed that neuroinvasion can occur through various mechanisms (55–59). Following i.p. administration, it has been shown through temporal studies that the infectious agent most likely gains access to the spinal cord and midbrain through retrograde axonal transport via the parasympathetic and sympathetic innervation of the enteric nervous system in the gut (55, 56). Neuroinvasion following intravenous injection of the infectious prion agent is thought to occur through circumventricular organs as a result of a deficient blood-brain barrier at these sites (57, 58) and may involve transport by hematopoietic cells to secondary lymphoid organs and uptake by nerve endings in these organs (59). Future studies will focus on understanding whether such mechanisms apply to αS transmission.

MATERIALS AND METHODS

αS transgenic mice, husbandry, and injections. All procedures were performed according to the *Guide for the Care and Use of Laboratory Animals* (60) and were approved by the University of Florida Institutional Animal Care and Use Committee. M83 Tg mice expressing human αS with the A53T mutation or M20 Tg mice expressing wild-type human αS driven by the mouse prion protein promoter were previously described (41, 49). M83 and M20 Tg mice both express endogenous mouse αS. M83$^{+/+}$ mice, which have two alleles of the genetically inserted transgene, overexpress approximately 5-fold human αS in the brain cortex and 28-fold human αS in the spinal cord relative to endogenous mouse αS (41). The overall levels of human αS throughout the neuroaxis in these mice is about the same, but the differences relative to endogenous levels are mostly due to the lower levels of endogenous mouse αS in the spinal cord (41, 61). In comparison, M83$^{+/-}$ mice overexpress approximately 3-fold human αS in the brain cortex and 19-fold human αS in the spinal cord relative to endogenous mouse αS (41). M20$^{+/-}$ mice overexpress approximately 6-fold human αS in the brain cortex and 28-fold human αS in the spinal cord relative to endogenous mouse αS (41).

Antibodies. pSer129 clone 81A is a mouse monoclonal antibody that reacts with αS phosphorylated at Ser129 (pSer129) (62), but also cross-reacts with phosphorylated low-molecular-mass neurofilament subunit (63). The rabbit monoclonal antibody pSer129/EP1536Y that reacts with αS phosphorylated at Ser129 and does not cross-react with phosphorylated low-molecular-mass neurofilament subunit (6) was obtained from Abcam (Cambridge, MA). Syn506 is a conformational anti-αS mouse monoclonal antibody that preferentially detects αS in pathological inclusions (64, 65). A rabbit anti-p62/sequestosome polyclonal antibody (SQSTM1) was obtained from Proteintech (Chicago, IL).

Histology. Mice were sacrificed by CO_2 euthanization and perfused with phosphate-buffered saline (PBS)–heparin. The brain and spinal cord were then removed and fixed with 70% ethanol–150 mM NaCl for at least 48 h. As previously described, tissue samples were dehydrated at room temperature by immersion in a series of ethanol solutions and then xylene and then infiltration with paraffin at 60°C (66). The tissue samples were then embedded into paraffin blocks, which were cut into 6-μm sections. Immunostaining of the sections was performed using previously described methods (66) using the avidin-biotin complex (ABC) system (Vectastain ABC Elite kit; Vector Laboratories, Burlingame, CA), and immunocomplexes were visualized with the chromogen 3,3′-diaminobenzidine (DAB kit; KPL, Gaithersburg, MD). Sections were counterstained with hematoxylin. All slides were scanned using an Aperio ScanScope CS instrument (40× magnification; Aperio Technologies Inc., Vista, CA), and images of representative areas of αS pathology were taken using the ImageScope software (40× magnification; Aperio Technologies Inc.).

Silver staining of tissues was achieved using an adapted version of the Campbell-Switzer silver stain protocol (67). Briefly, tissue sections were treated with 2% ammonium hydroxide, rinsed in water, then placed in silver-pyridine-carbonate solution (0.5% silver nitrate, 0.4% potassium carbonate, 0.14% pyridine) for 40 min in the dark. The slides were then soaked in 1% citric acid, washed in acetate buffer (50 mM acetic acid, 50 mM sodium acetate [pH 5.0]) and developed in developer solution (236 mM silver carbonate, 12.5 mM ammonium nitrate, 6 mM silver nitrate, 29.4 mM tungstosilicic acid) following the addition of 0.025% formaldehyde. The slides were washed in 0.5% sodium thiosulfate and water and then dehydrated, and cover slips were placed over the slides.

Expression and purification of recombinant αS proteins. Recombinant full-length human and mouse αS, 71-82 deletion (Δ71-82) human αS, and full-length human βS were expressed and purified to homogeneity as previously described (42, 43, 68). Δ71-82 αS has a deletion in the middle of the hydrophobic region of αS that is required for amyloid formation and therefore lacks the ability to form or seed αS amyloid *in vitro* and *in vivo* under physiological conditions (42–45). Nonaggregated, soluble αS was centrifuged at 100,000 × *g* for 1 h to remove possible aggregates just prior to injection.

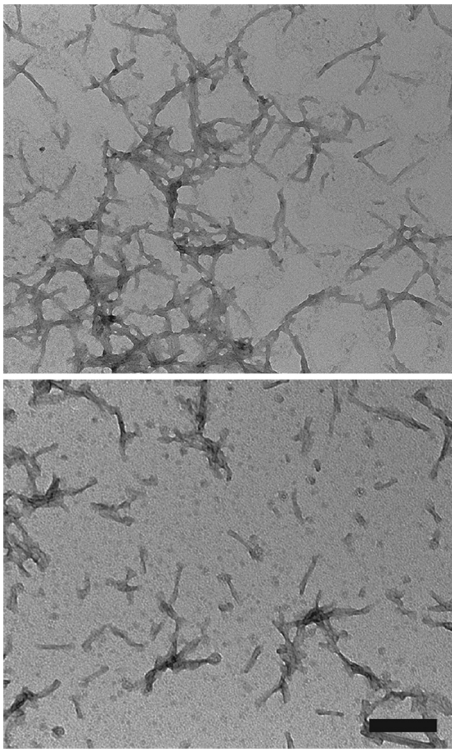

FIG 6 Negative staining electron microscopy of mouse αS fibs after water bath sonication. Representative images showing αS fibs that have been broken up into an array of polymers by water bath sonication. Grids were stained with 1% uranyl acetate. Bar = 200 nm.

Fibril preparation of recombinant αS for injection. Mouse αS was assembled into fibrils by incubation at 37°C at 5 mg/ml in sterile PBS (Invitrogen) with continuous shaking at 1,050 rpm (Thermomixer R; Eppendorf, Westbury, NY). αS amyloid fibril assembly was monitored as previously described with K114 fluorometry (43, 69). αS fibrils were diluted in sterile PBS and treated by mild water bath sonication for 1 h at room temperature. The presence of mouse αS fibs following the fibril formation assay was assessed by electron microscopy (EM) analysis (Fig. 6). These fibrils were tested for induction of intracellular amyloid inclusion formation as previously described (70).

Negative staining electron microscopy. Mouse αS was assembled into fibrils and sonicated as described above. Samples were adsorbed to 300-mesh carbon-coated copper grids, washed with PBS, and stained with 1% uranyl acetate. Images were captured using a Hitachi H7600 transmission electron microscope fitted with an AMT digital camera.

Intramuscular, intraperitoneal, and tail vein injections. Bilateral i.m. injections were conducted with 10 μg of protein listed in Table 2 per hind leg (20 μg total protein per mouse) in the gastrocnemius muscle as previously described (40). Briefly, mice at 2 to 3 months of age were anesthetized with isoflurane (1 to 5%) inhalation, the back of the hind limbs were shaved, and a 10-μl Hamilton syringe with a 30-gauge needle was inserted into the muscle. Different syringes were used for each type of inoculum to prevent any contamination. Intraperitoneal injections were conducted with 50 μg of proteins listed in Table 1 in 100 μl of sterile PBS. For tail vein injections, mice were injected with 20 μg of mouse αS fibs in 100 μl PBS using a 26-gauge needle. Mice were monitored for the onset of hind limb motor impairment, and the percent motor impaired was calculated as the number of mice displaying motor impairment divided by the number of total mice injected for that particular cohort.

ACKNOWLEDGMENTS

This work was supported by grants from the National Institute of Neurological Disorders and Stroke (NINDS) (NS089622) and the National Parkinson Foundation (NPF-UN203). The authors have no conflict of interest.

REFERENCES

1. Waxman EA, Giasson BI. 2009. Molecular mechanisms of alpha-synuclein neurodegeneration. Biochim Biophys Acta 1792:616–624. https://doi.org/10.1016/j.bbadis.2008.09.013.
2. Goedert M. 1997. Familial Parkinson's disease. The awakening of alpha-synuclein. Nature 388:232–233.
3. Goedert M. 2001. Alpha-synuclein and neurodegenerative diseases. Nat Rev Neurosci 2:492–501. https://doi.org/10.1038/35081564.
4. Cookson MR. 2005. The biochemistry of Parkinson's disease. Annu Rev Biochem 74:29–52. https://doi.org/10.1146/annurev.biochem.74.082803.133400.

5. Goedert M, Spillantini MG, Del Tredici K, Braak H. 2013. 100 years of Lewy pathology. Nat Rev Neurol 9:13–24. https://doi.org/10.1038/nrneurol.2012.242.
6. Uchihara T, Giasson BI. 2016. Propagation of alpha-synuclein pathology: hypotheses, discoveries, and yet unresolved questions from experimental and human brain studies. Acta Neuropathol 131:49–73. https://doi.org/10.1007/s00401-015-1485-1.
7. Spillantini MG, Schmidt ML, Lee VM-Y, Trojanowski JQ, Jakes R, Goedert M. 1997. Alpha-synuclein in Lewy bodies. Nature 388:839–840. https://doi.org/10.1038/42166.
8. Lantos PL. 1997. Multiple system atrophy. Brain Pathol 7:1293–1297. https://doi.org/10.1111/j.1750-3639.1997.tb01034.x.
9. Tu PH, Galvin JE, Baba M, Giasson B, Tomita T, Leight S, Nakajo S, Iwatsubo T, Trojanowski JQ, Lee VM-Y. 1998. Glial cytoplasmic inclusions in white matter oligodendrocytes of multiple system atrophy brains contain insoluble alpha-synuclein. Ann Neurol 44:415–422. https://doi.org/10.1002/ana.410440324.
10. Spillantini MG, Crowther RA, Jakes R, Cairns NJ, Lantos PL, Goedert M. 1998. Filamentous alpha-synuclein inclusions link multiple system atrophy with Parkinson's disease and dementia with Lewy bodies. Neurosci Lett 251:205–208. https://doi.org/10.1016/S0304-3940(98)00504-7.
11. Appel-Cresswell S, Vilarino-Guell C, Encarnacion M, Sherman H, Yu I, Shah B, Weir D, Thompson C, Szu-Tu C, Trinh J, Aasly JO, Rajput A, Rajput AH, Jon SA, Farrer MJ. 2013. Alpha-synuclein p.H50Q, a novel pathogenic mutation for Parkinson's disease. Mov Disord 28:811–813. https://doi.org/10.1002/mds.25421.
12. Kiely AP, Asi YT, Kara E, Limousin P, Ling H, Lewis P, Proukakis C, Quinn N, Lees AJ, Hardy J, Revesz T, Houlden H, Holton JL. 2013. Alpha-synucleinopathy associated with G51D SNCA mutation: a link between Parkinson's disease and multiple system atrophy? Acta Neuropathol 125:753–769. https://doi.org/10.1007/s00401-013-1096-7.
13. Kruger R, Kuhn W, Muller T, Woitalla D, Graeber M, Kosel S, Przuntek H, Epplen JT, Schols L, Riess O. 1998. Ala30Pro mutation in the gene encoding alpha-synuclein in Parkinson's disease. Nat Genet 18:106–108. https://doi.org/10.1038/ng0298-106.
14. Lesage S, Anheim M, Letournel F, Bousset L, Honore A, Rozas N, Pieri L, Madiona K, Durr A, Melki R, Verny C, Brice A, French Parkinson's Disease Genetics Study Group. 2013. G51D alpha-synuclein mutation causes a novel parkinsonian-pyramidal syndrome. Ann Neurol 73:459–471. https://doi.org/10.1002/ana.23894.
15. Pasanen P, Myllykangas L, Siitonen M, Raunio A, Kaakkola S, Lyytinen J, Tienari PJ, Poyhonen M, Paetau A. 2014. Novel alpha-synuclein mutation A53E associated with atypical multiple system atrophy and Parkinson's disease-type pathology. Neurobiol Aging 35:2180.e1–2180.e5. https://doi.org/10.1016/j.neurobiolaging.2014.03.024.
16. Proukakis C, Dudzik CG, Brier T, Mackay DS, Cooper JM, Millhauser GL, Houlden H, Schapira AH. 2013. A novel alpha-synuclein missense mutation in Parkinson disease. Neurology 80:1062–1064. https://doi.org/10.1212/WNL.0b013e31828727ba.
17. Zarranz JJ, Alegre J, Gomez-Esteban JC, Lezcano E, Ros R, Ampuero I, Vidal L, Hoenicka J, Rodriguez O, Atares B, Llorens V, Gomez TE, del Ser T, Munoz DG, de Yebenes JG. 2004. The new mutation, E46K, of alpha-synuclein causes Parkinson and Lewy body dementia. Ann Neurol 55:164–173. https://doi.org/10.1002/ana.10795.
18. Chartier-Harlin MC, Kachergus J, Roumier C, Mouroux V, Douay X, Lincoln S, Levecque C, Larvor L, Andrieux J, Hulihan M, Waucquier N, Defebvre L, Amouyel P, Farrer M, Destee A. 2004. Alpha-synuclein locus duplication as a cause of familial Parkinson's disease. Lancet 364:1167–1169. https://doi.org/10.1016/S0140-6736(04)17103-1.
19. Farrer M, Kachergus J, Forno L, Lincoln S, Wang DS, Hulihan M, Maraganore D, Gwinn-Hardy K, Wszolek Z, Dickson D, Langston JW. 2004. Comparison of kindreds with parkinsonism and alpha-synuclein genomic multiplications. Ann Neurol 55:174–179. https://doi.org/10.1002/ana.10846.
20. Singleton AB, Farrer M, Johnson J, Singleton A, Hague S, Kachergus J, Hulihan M, Peuralinna T, Dutra A, Nussbaum R, Lincoln S, Crawley A, Hanson M, Maraganore D, Adler C, Cookson MR, Muenter M, Baptista M, Miller D, Blancato J, Hardy J, Gwinn-Hardy K. 2003. Alpha-synuclein locus triplication causes Parkinson's disease. Science 302:841. https://doi.org/10.1126/science.1090278.
21. Polymeropoulos MH, Lavedan C, Leroy E, Ide SE, Dehejia A, Dutra A, Pike B, Root H, Rubenstein J, Boyer R, Stenroos ES, Chandrasekharappa S, Athanassiadou A, Papapetropoulos T, Johnson WG, Lazzarini AM, Duvoisin RC, Di Iorio G, Golbe LI, Nussbaum RL. 1997. Mutation in the alpha-synuclein gene identified in families with Parkinson's disease. Science 276:2045–2047. https://doi.org/10.1126/science.276.5321.2045.
22. Braak H, Bohl JR, Muller CM, Rub U, de Vos RA, Del Tredici K. 2006. Stanley Fahn Lecture 2005: the staging procedure for the inclusion body pathology associated with sporadic Parkinson's disease reconsidered. Mov Disord 21:2042–2051. https://doi.org/10.1002/mds.21065.
23. Braak H, Del Tredici K, Rub U, de Vos RA, Jansen Steur EN, Braak E. 2003. Staging of brain pathology related to sporadic Parkinson's disease. Neurobiol Aging 24:197–211. https://doi.org/10.1016/S0197-4580(02)00065-9.
24. Braak H, Rub U, Gai WP, Del Tredici K. 2003. Idiopathic Parkinson's disease: possible routes by which vulnerable neuronal types may be subject to neuroinvasion by an unknown pathogen. J Neural Transm 110:517–536. https://doi.org/10.1007/s00702-002-0808-2.
25. Braak H, de Vos RA, Bohl J, Del Tredici K. 2006. Gastric alpha-synuclein immunoreactive inclusions in Meissner's and Auerbach's plexuses in cases staged for Parkinson's disease-related brain pathology. Neurosci Lett 396:67–72. https://doi.org/10.1016/j.neulet.2005.11.012.
26. Wakabayashi K, Mori F, Tanji K, Orimo S, Takahashi H. 2010. Involvement of the peripheral nervous system in synucleinopathies, tauopathies and other neurodegenerative proteinopathies of the brain. Acta Neuropathol 120:1–12. https://doi.org/10.1007/s00401-010-0706-x.
27. Luk KC, Kehm V, Carroll J, Zhang B, O'Brien P, Trojanowski JQ, Lee VM. 2012. Pathological alpha-synuclein transmission initiates Parkinson-like neurodegeneration in nontransgenic mice. Science 338:949–953. https://doi.org/10.1126/science.1227157.
28. Luk KC, Kehm VM, Zhang B, O'Brien P, Trojanowski JQ, Lee VM. 2012. Intracerebral inoculation of pathological alpha-synuclein initiates a rapidly progressive neurodegenerative alpha-synucleinopathy in mice. J Exp Med 209:975–986. https://doi.org/10.1084/jem.20112457.
29. Prusiner SB, Woerman AL, Mordes DA, Watts JC, Rampersaud R, Berry DB, Patel S, Oehler A, Lowe JK, Kravitz SN, Geschwind DH, Glidden DV, Halliday GM, Middleton LT, Gentleman SM, Grinberg LT, Giles K. 2015. Evidence for alpha-synuclein prions causing multiple system atrophy in humans with parkinsonism. Proc Natl Acad Sci U S A 112:E5308–E5317. https://doi.org/10.1073/pnas.1514475112.
30. Watts JC, Giles K, Oehler A, Middleton L, Dexter DT, Gentleman SM, DeArmond SJ, Prusiner SB. 2013. Transmission of multiple system atrophy prions to transgenic mice. Proc Natl Acad Sci USA 110:19555–19560. https://doi.org/10.1073/pnas.1318268110.
31. Woerman AL, Stohr J, Aoyagi A, Rampersaud R, Krejciova Z, Watts JC, Ohyama T, Patel S, Widjaja K, Oehler A, Sanders DW, Diamond MI, Seeley WW, Middleton LT, Gentleman SM, Mordes DA, Sudhof TC, Giles K, Prusiner SB. 2015. Propagation of prions causing synucleinopathies in cultured cells. Proc Natl Acad Sci U S A 112:E4949–E4958. https://doi.org/10.1073/pnas.1513426112.
32. Mougenot AL, Nicot S, Bencsik A, Morignat E, Verchere J, Lakhdar L, Legastelois S, Baron T. 2012. Prion-like acceleration of a synucleinopathy in a transgenic mouse model. Neurobiol Aging 33:2225–2228. https://doi.org/10.1016/j.neurobiolaging.2011.06.022.
33. Masuda-Suzukake M, Nonaka T, Hosokawa M, Kubo M, Shimozawa A, Akiyama H, Hasegawa M. 2014. Pathological alpha-synuclein propagates through neural networks. Acta Neuropathol Commun 2:88. https://doi.org/10.1186/s40478-014-0088-8.
34. Masuda-Suzukake M, Nonaka T, Hosokawa M, Oikawa T, Arai T, Akiyama H, Mann DM, Hasegawa M. 2013. Prion-like spreading of pathological alpha-synuclein in brain. Brain 136:1128–1138. https://doi.org/10.1093/brain/awt037.
35. Rutherford NJ, Sacino AN, Brooks M, Ceballos-Diaz C, Ladd TB, Howard JK, Golde TE, Giasson BI. 2015. Studies of lipopolysaccharide effects on the induction of alpha-synuclein pathology by exogenous fibrils in transgenic mice. Mol Neurodegener 10:32. https://doi.org/10.1186/s13024-015-0029-4.
36. Sacino AN, Brooks M, McGarvey NH, McKinney AB, Thomas MA, Levites Y, Ran Y, Golde TE, Giasson BI. 2013. Induction of CNS alpha-synuclein pathology by fibrillar and non-amyloidogenic recombinant alpha-synuclein. Acta Neuropathol Commun 1:38. https://doi.org/10.1186/2051-5960-1-38.
37. Sacino AN, Brooks M, McKinney AB, Thomas MA, Shaw G, Golde TE, Giasson BI. 2014. Brain injection of alpha-synuclein induces multiple proteinopathies, gliosis, and a neuronal injury marker. J Neurosci 34:12368–12378. https://doi.org/10.1523/JNEUROSCI.2102-14.2014.
38. Betemps D, Verchere J, Brot S, Morignat E, Bousset L, Gaillard D, Lakhdar L, Melki R, Baron T. 2014. Alpha-synuclein spreading in M83 mice brain revealed by detection of pathological alpha-synuclein by enhanced

ELISA. Acta Neuropathol Commun 2:29. https://doi.org/10.1186/2051-5960-2-29.
39. Sacino AN, Ayers JI, Brooks MM, Chakrabarty P, Hudson VJ, III, Howard JK, Golde TE, Giasson BI, Borchelt DR. 2016. Non-prion-type transmission in A53T alpha-synuclein transgenic mice: a normal component of spinal homogenates from naive non-transgenic mice induces robust alpha-synuclein pathology. Acta Neuropathol 131:151–154. https://doi.org/10.1007/s00401-015-1505-1.
40. Sacino AN, Brooks M, Thomas MA, McKinney AB, Lee S, Regenhardt RW, McGarvey NH, Ayers JI, Notterpek L, Borchelt DR, Golde TE, Giasson BI. 2014. Intramuscular injection of alpha-synuclein induces CNS alpha-synuclein pathology and a rapid-onset motor phenotype in transgenic mice. Proc Natl Acad Sci USA 111:10732–10737. https://doi.org/10.1073/pnas.1321785111.
41. Giasson BI, Duda JE, Quinn SM, Zhang B, Trojanoswki JQ, Lee VM-Y. 2002. Neuronal α-synucleinopathy with severe movement disorder in mice expressing A53T human α-synuclein. Neuron 34:521–533. https://doi.org/10.1016/S0896-6273(02)00682-7.
42. Giasson BI, Murray IV, Trojanowski JQ, Lee VM-Y. 2001. A hydrophobic stretch of 12 amino acid residues in the middle of alpha-synuclein is essential for filament assembly. J Biol Chem 276:2380–2386. https://doi.org/10.1074/jbc.M008919200.
43. Waxman EA, Mazzulli JR, Giasson BI. 2009. Characterization of hydrophobic residue requirements for alpha-synuclein fibrillization. Biochemistry 48:9427–9436. https://doi.org/10.1021/bi900539p.
44. Luk KC, Song C, O'Brien P, Stieber A, Branch JR, Brunden KR, Trojanowski JQ, Lee VM. 2009. Exogenous alpha-synuclein fibrils seed the formation of Lewy body-like intracellular inclusions in cultured cells. Proc Natl Acad Sci USA 106:20051–20056. https://doi.org/10.1073/pnas.0908005106.
45. Sacino AN, Thomas MA, Ceballos-Diaz C, Cruz PE, Rosario AM, Lewis J, Giasson BI, Golde TE. 2013. Conformational templating of alpha-synuclein aggregates in neuronal-glial cultures. Mol Neurodegener 8:17. https://doi.org/10.1186/1750-1326-8-17.
46. George JM. 2002. The synucleins. Genome Biol 3:REVIEWS3002.
47. Spillantini MG, Crowther RA, Jakes R, Hasegawa M, Goedert M. 1998. Alpha-synuclein in filamentous inclusions of Lewy bodies from Parkinson's disease and dementia with Lewy bodies. Proc Natl Acad Sci USA 95:6469–6473. https://doi.org/10.1073/pnas.95.11.6469.
48. Zibaee S, Fraser G, Jakes R, Owen D, Serpell LC, Crowther RA, Goedert M. 2010. Human beta-synuclein rendered fibrillogenic by designed mutations. J Biol Chem 285:38555–38567. https://doi.org/10.1074/jbc.M110.160721.
49. Emmer KL, Waxman EA, Covy JP, Giasson BI. 2011. E46K human alpha-synuclein transgenic mice develop Lewy-like and tau pathology associated with age-dependent, detrimental motor impairment. J Biol Chem 286:35104–35118. https://doi.org/10.1074/jbc.M111.247965.
50. Breid S, Bernis ME, Babila JT, Garca MC, Wille H, Tamguney G. 2016. Neuroinvasion of alpha-synuclein prionoids after intraperitoneal and intraglossal inoculation. J Virol 90:9182–9193. https://doi.org/10.1128/JVI.01399-16.
51. Rivers RC, Kumita JR, Tartaglia GG, Dedmon MM, Pawar A, Vendruscolo M, Dobson CM, Christodoulou J. 2008. Molecular determinants of the aggregation behavior of alpha- and beta-synuclein. Protein Sci 17:887–898. https://doi.org/10.1110/ps.073181508.
52. Golde TE, Borchelt DR, Giasson BI, Lewis J. 2013. Thinking laterally about neurodegenerative proteinopathies. J Clin Invest 123:1847–1855. https://doi.org/10.1172/JCI66029.
53. Brundin P, Li JY, Holton JL, Lindvall O, Revesz T. 2008. Research in motion: the enigma of Parkinson's disease pathology spread. Nat Rev Neurosci 9:741–745. https://doi.org/10.1038/nrn2477.
54. Peelaerts W, Bousset L, Van der Perren A, Moskalyuk A, Pulizzi R, Giugliano M, Van den Haute C, Melki R, Baekelandt V. 2015. Alpha-synuclein strains cause distinct synucleinopathies after local and systemic administration. Nature 522:340–344. https://doi.org/10.1038/nature14547.
55. Beekes M, McBride PA. 2000. Early accumulation of pathological PrP in the enteric nervous system and gut-associated lymphoid tissue of hamsters orally infected with scrapie. Neurosci Lett 278:181–184. https://doi.org/10.1016/S0304-3940(99)00934-9.
56. McBride PA, Schulz-Schaeffer WJ, Donaldson M, Bruce M, Diringer H, Kretzschmar HA, Beekes M. 2001. Early spread of scrapie from the gastrointestinal tract to the central nervous system involves autonomic fibers of the splanchnic and vagus nerves. J Virol 75:9320–9327. https://doi.org/10.1128/JVI.75.19.9320-9327.2001.
57. Siso S, Jeffrey M, Gonzalez L. 2009. Neuroinvasion in sheep transmissible spongiform encephalopathies: the role of the haematogenous route. Neuropathol Appl Neurobiol 35:232–246. https://doi.org/10.1111/j.1365-2990.2008.00978.x.
58. Siso S, Jeffrey M, Martin S, Houston F, Hunter N, Gonzalez L. 2009. Pathogenetical significance of porencephalic lesions associated with intracerebral inoculation of sheep with the bovine spongiform encephalopathy (BSE) agent. Neuropathol Appl Neurobiol 35:247–258. https://doi.org/10.1111/j.1365-2990.2009.01013.x.
59. Aguzzi A, Sigurdson C, Heikenwaelder M. 2008. Molecular mechanisms of prion pathogenesis. Annu Rev Pathol 3:11–40. https://doi.org/10.1146/annurev.pathmechdis.3.121806.154326.
60. National Research Council. 2011. Guide for the care and use of laboratory animals, 8th ed. National Academies Press, Washington, DC.
61. Giasson BI, Duda JE, Forman MS, Lee VM-Y, Trojanoswki JQ. 2001. Prominent perikaryal expression of α- and β-synuclein in neurons of dorsal root ganglion and in medullary neurons. Exp Neurol 172:354–362. https://doi.org/10.1006/exnr.2001.7805.
62. Waxman EA, Giasson BI. 2008. Specificity and regulation of casein kinase-mediated phosphorylation of alpha-synuclein. J Neuropathol Exp Neurol 67:402–416. https://doi.org/10.1097/NEN.0b013e3186fc995.
63. Sacino AN, Brooks M, Thomas MA, McKinney AB, McGarvey NH, Rutherford NJ, Ceballos-Diaz C, Robertson J, Golde TE, Giasson BI. 2014. Amyloidogenic alpha-synuclein seeds do not invariably induce rapid, widespread pathology in mice. Acta Neuropathol 127:645–665. https://doi.org/10.1007/s00401-014-1268-0.
64. Duda JE, Giasson BI, Mabon ME, Lee VM-Y, Trojanoswki JQ. 2002. Novel antibodies to oxidized α-synuclein reveal abundant neuritic pathology in Lewy body disease. Ann Neurol 52:205–210. https://doi.org/10.1002/ana.10279.
65. Waxman EA, Duda JE, Giasson BI. 2008. Characterization of antibodies that selectively detect alpha-synuclein in pathological inclusions. Acta Neuropathol 116:37–46. https://doi.org/10.1007/s00401-008-0375-1.
66. Duda JE, Giasson BI, Gur TL, Montine TJ, Robertson D, Biaggioni I, Hurtig HI, Stern MB, Gollomp SM, Grossman M, Lee VM-Y, Trojanowski JQ. 2000. Immunohistochemical and biochemical studies demonstrate a distinct profile of alpha-synuclein permutations in multiple system atrophy. J Neuropathol Exp Neurol 59:830–841. https://doi.org/10.1093/jnen/59.9.830.
67. Vallet PG, Guntern R, Hof PR, Golaz J, Delacourte A, Robakis NK, Bouras C. 1992. A comparative study of histological and immunohistochemical methods for neurofibrillary tangles and senile plaques in Alzheimer's disease. Acta Neuropathol 83:170–178. https://doi.org/10.1007/BF00308476.
68. Greenbaum EA, Graves CL, Mishizen-Eberz AJ, Lupoli MA, Lynch DR, Englander SW, Axelsen PH, Giasson BI. 2005. The E46K mutation in alpha-synuclein increases amyloid fibril formation. J Biol Chem 280:7800–7807. https://doi.org/10.1074/jbc.M411638200.
69. Crystal AS, Giasson BI, Crowe A, Kung MP, Zhuang ZP, Trojanowski JQ, Lee VM. 2003. A comparison of amyloid fibrillogenesis using the novel fluorescent compound K114. J Neurochem 86:1359–1368. https://doi.org/10.1046/j.1471-4159.2003.01949.x.
70. Waxman EA, Giasson BI. 2010. A novel, high-efficiency cellular model of fibrillar alpha-synuclein inclusions and the examination of mutations that inhibit amyloid formation. J Neurochem 113:374–388. https://doi.org/10.1111/j.1471-4159.2010.06592.x.